The Influence of Gravity-adapted Target Resizing on Direct Augmented Reality Pointing under Simulated Hypergravity

Daniela Markov-Vetter[1,3], Vanja Zander[2], Joachim Latsch[2] and Oliver Staadt[3]
[1]*Institute Aerospace Medicine, German Aersospace Center, Cologne, Germany*
[2]*Institute of Cardiology and Sports Medicine, German Sport University Cologne, Cologne, Germany*
[3]*Institute of Computer Science, University of Rostock, Rostock, Germany*

Keywords: Augmented Reality, Interaction, Direct Pointing, Usability.

Abstract: The performance of Augmented Reality direct object selection coded outside of the human egocentric body frame of reference decreases under short-term altered gravity. Therefore adequate countermeasures are required. This paper presents the results of a proof-of-concept (POC) study to investigate the impact of simulated hypergravity on the size and distance of a given target. The POC study is divided in a case study and a user study, whereby hypergravity was induced by a long-arm human centrifuge and additional arm weighting. For gravity-dependent resizing and –positioning we used the Hooke's law that resulted in two techniques of target deformation (compression, elongation) and compared both methods with normal sized targets. Besides common metrics to measure the performance, we additionally evaluated the physiological strain by the heart rate variability and the speed-accuracy tradeoff of the resizing techniques according to Fitts' law. The study showed that the online adaption of the present gravity load to targets' size and distance influences the performance of direct AR direct pointing. The results revealed that the pointing performance benefits from elongation target deformation by increased target sizes and distances.

1 INTRODUCTION

Advanced concepts of user interfaces are shifting away from conventional displays and input devices and claim more integration into our physical world. Augmented Reality (AR) (Azuma, 1997) keeps the natural perception and offers a direct interface by merging 3D-registered virtual information with the real world in real time. Current research on human factors of handling AR interfaces presumes the application under normogravity (1*g*) condition on Earth. The application of AR to intra-vehicular space operations could support astronauts in their procedural task performance at complex technical facilities aboard the International Space Station (ISS) (Agan et al., 1998; Scheid et al., 2010).

In early prototyping and evaluation of an AR-supported assistance system for standardized space operations (Markov-Vetter et al., 2013) we could show the feasibility and acceptance of domain experts. For ensuring successful user performance the integration of environmental factors into the design processes is required. The adaption of human-computer interaction to weightlessness is a challenge that strongly affects the level of usability. Working under altered gravity not only results in an increased workload of user performance, it also denotes changes in human sensorimotor coordination (Bock et al., 1998), especially in aimed pointing movements (Fisk et al., 1993; Bock et al., 1992). Previous studies under parabolic flight (PF) conditions (Markov-Vetter et al., 2012) have shown that head-mounted AR interfaces for symbolic input tasks (e.g., AR soft keyboard) under short-term hyper- and microgravity conditions requires haptic feedback and should be coded inside of human's egocentric body frame of reference (e.g., attached to limbs). Despite these results, the future main application of an AR supported guidance system is predominantly coded outside of the user's body frame. Therefore, we are investigating adequate countermeasures to maintain user performance in object selection tasks as under those conditions. In general, the selection performance can be affected for example by targets' size and distance. Looser et al. (2007) evaluated different AR selection techniques (Direct Touch, Ray-Casting, Magic Lens) for different predefined target sizes, target density

Markov-Vetter D., Zander V., Latsch J. and Staadt O..
The Influence of Gravity-adapted Target Resizing on Direct Augmented Reality Pointing under Simulated Hypergravity.
DOI: 10.5220/0005316604010411
In *Proceedings of the 10th International Conference on Computer Graphics Theory and Applications* (GRAPP-2015), pages 401-411
ISBN: 978-989-758-087-1

and distance to the users. In contrast to that, we used a contrary approach for the evaluation of gravity-adapted targets' size and position. We used only a direct touch interface for object selection in a head-mounted AR environment. We hypothesize that: (1) increased gravity conditions decrease the pointing performance towards normal sized targets, and (2) gravity-adapted target resizing impacts the performance and workload of direct AR pointing.

Before conducting expensive experiments under simulated weightlessness conditions (e.g., parabolic flight), we performed a proof-of-concept (POC) study under simulated hypergravity (+Gz) conditions. We predicted variations of the pointing performance (e.g., response time, speed, etc.) correlated to the resized and -positioned information visualisation depends on the adapted gravity force. In response to visual stimuli the participant should point towards virtual targets under altered +Gz loads while wearing an optical see-through head-mounted display (OST HMD). Until now, there have been no equivalent studies on gravity-based target resizing and -positioning conducted under simulated hypergravity. The POC study was divided into two parts using different simulations of hypergravity. Firstly, we performed a case study where +Gz load was induced by a long-arm human centrifuge and pointing towards an AR soft keyboard for the experimentation task. Secondly, we performed an experiment under normogravity and simulated +Gz load by additional arm weighting (Guardiera et al., 2008) as validated method. To evaluate the performance during the weight study we considered the international standard for pointing devices (ISO/DIS 9241-9, 2000) using the Fitts' multi-directional tapping task (MacKenzie, 1992). There have been only few studies applying Fitts' law on evaluation of AR interaction (Rohs et al., 2011), or on head-mounted Mixed Reality pointing (Kohli et al., 2012).

Measuring the performance of aimed pointing includes metrics such as the frequency of correct and incorrect pointing, the accuracy, the response time and the pointing speed. Since the physiological factor is essential in sensorimotor coordination, we recorded and evaluated the physiological strain by assessing the heart rate variability (HRV) (Tümler et al., 2008; Oehme et al., 2002) in the weight study. This is an immanent expression of sympathetic and parasympathetic influences of the function of the heart (Task Force, 1996).

In the next section, the gravity adapted sizing technique that were used for both experiments is presented. The following sections describe the case study and weighting experiments. We finally discuss the results and suggest future research.

2 THE FORCE-BASED SIZING

For improving the performance of aimed pointing movements towards virtual targets under altered gravity conditions, we use a force-based approach for automated transformation of the targets. Force-based approaches are typically used for automated positioning of labels and annotations, e.g. in 3D information visualization (Pick et al., 2010; Hartmann et al., 2004). Depending on the present gravity load we calculate a corresponding force affecting target's size and position. Our approach for target resizing and -positioning is derived from the elastic behaviour of soft bodies, which are proportional deformed to the applied gravity load G_{sim}, similar to Hooke's law (Eq. 1). Therefore, we calculated the axial (Eq. 2) and transversal (Eq. 3) strain of the target using empirical values for the modulus of elasticity E and Poisson's ratio v. Thereby, we distinguished between two techniques of target sizing – sizing by compression (SC, Eq. 4) and sizing by elongation (SE, Eq. 5). Their output was compared with the unmodified sizing technique (SU) as baseline condition that does not affect the targets. For first experimentation we limited the evaluated parameters by automated target resizing without the transversal strain Δw, but applied the axial strain Δh proportionally to target's height and width. Figure 1 shows the resulted sizing techniques that we have investigated. We also applied the gravity-based changes to the complete interface, i.e. to targets' position. That resulted in larger target distance with the SE technique and in smaller distances with the compressed SC technique. While the SC sizing technique provides smaller targets and benefits from smaller target distances, the SE technique offers larger target size at larger distance. Therewith, we evaluated the efficiency of sensorimotor coordination during direct AR pointing tasks. To our knowledge, gravity-adapted target sizing was not reported until now.

$$\sigma = E\varepsilon \quad \text{with} \quad \varepsilon = \frac{\Delta h}{h} \quad \text{and} \quad \sigma = \frac{F}{A} \tag{1}$$

$$\Delta h = \frac{F * h}{A * E} \quad \text{with} \quad A = h^2 \quad \text{and} \quad F = G_{sim} \tag{2}$$

$$\Delta w = -w * v\frac{\Delta h}{h} \tag{3}$$

$$h_{SC} = h - \Delta h\,, \quad w_{SC} = w - \Delta w \tag{4}$$

$$h_{SE} = h + \Delta h\,, \quad w_{SE} = w + \Delta w \tag{5}$$

For designing the normal sized targets (SU) we followed the recommended ergonomic size range for push buttons (Department of Defense. 1999) and used a squared target of 15mm width and height for the unmodified method.

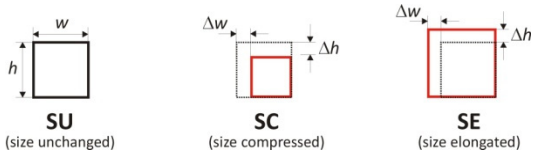

Figure 1: Methods of target sizing being evaluated.

3 CASE STUDY BY LONG-ARM HUMAN CENTRIFUGE (LAHC)

To proof our concept of the gravity-adapted approach initially, we were allowed to perform a case study under +Gz load induced by a long-arm human centrifuge (LAHC, see Fig. 2). Human centrifuges enable research in medicine and human physiology during altered +Gz load and are also used to train pilots and astronauts. The case study was performed with one participant. The male participant (51 years old, space engineer) is very experienced under altered +Gz load (human centrifuge, parabolic flight) and familiarized with the used AR pointing system and task.

3.1 Apparatus

We used a right-sided monocular optical see-through head mounted display (OST HMD, Shimadzu dataGlass2/a), which has a semi-transparent LCD display with a resolution of 800x600 pixels and a diagonal field of view (FOV) of 30 degrees (see Fig. 3, left). The HMD was connected to the data processing unit (Lenovo ThinkPad T420s, 2.8 GHz CPU, NVIDIA Quadro NVS 4200M), which was installed under the participant's seat in the centrifuge cabin. For optical inside-out marker tracking we equipped the HMD with an optical sensor (Microsoft HD 5000 webcam with 66 degree diagonal FOV). To compute the position of participant's eye relative to the optical sensor, the participant had to perform a self-calibration (Kato et al., 1999). To realize pointing with haptic feedback we used a panel that was installed in front of the participant and was equipped with a multi-marker configuration. For the pointing purpose a single marker was attached to the participant's fingertip at the dominant hand. The pose data were captured with a mean frame rate of 38.74 fps (SD = 10.05) by the optical sensor at constant artificial light conditions.

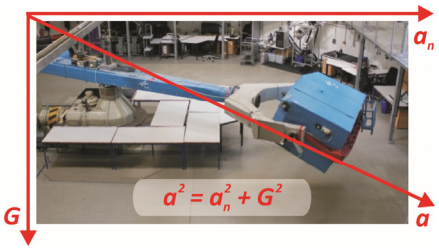

Figure 2: Used LAHC (5 m radius) with centrifugal acceleration a_n. The cabin is swinging out during the rotation with resulted acceleration a in line with subject's long body axis.

3.2 Experiment Task

Pointing in response to visual stimuli was done based on the PF experiment task (Markov-Vetter et al., 2012) by using a soft AR keyboard with squared keys of 15mm width and height (Department of Defense. 1999). The participant was requested to enter prescribed random pseudo-letters on the virtual keyboard (see Fig. 3, right). Entering letters onto the keyboard is determined by collision tests of a virtual ray ranging from the origin of the fingertip marker to the top of the index finger. The requested letter was signalled in green, hitting a correct key was highlighted in red and then the next key was signalled. Because the data processing unit was installed in the cabin of the centrifuge, the participant needed to start the experiment with a virtual start button displayed above the keyboard and hidden afterwards.

Figure 3: Participant sitting in the LAHC cabin, wearing the OST-HMD and pointing toward the panel *(left)*. The soft-AR keyboard (*right*).

3.3 Experiment Procedure

We conducted the experiment during three days. To perform the tasks, four randomized target pools were used per sizing technique. We defined a target pool as a pre-randomized series of keys. Pointing towards the keys of one target pool should be completed in 25 seconds. Within one centrifugation the participant performed the task for two sizing techniques (SC, SE) that resulted in a total pointing time of 200

seconds for each +Gz load. On the first day we tested only the feasibility and functionality. Because it was exhausting for the participant to perform arm movements for 200 s at one time, we reduced the operation time of a target pool to 20 s (in total 160 s per centrifugation) from the second day on. We distinguished between a fixed operation timer with 20 s runtime and a variable participant timer that was automatically started after entering the first key. If the operation timer elapsed, the timer for the participant was automatically stopped. To avoid transition effects between pool or method changes the first and the last signaled key where not recorded. Within one centrifugation the participant performed the task under one +Gz load using the unchanged method (SU) and one of the methods with force-based target sizing (SC, SE) in an alternated way. Thereby the sizing technique was changed after one target pool. We compared the methods SU with SC (second day) and SU and SE (third day) under 1.5*g*, 1.8*g* and 2.5*g* in a random presentation order. For reference purposes we also measured the pointing performance of the participant, using the SU method under 1*g* on the first day. For physiological regeneration and to avoid learning effects there was a 10 minutes break between the changes of the +Gz loads.

3.4 Results

Following we are showing the frequencies of correct and false target hits, the pointing response time in millisecond, the percentage error rate and the stroke rate per second. Thereby a false target hit constitutes that the participant entered a wrong key. The response time mirrors the elapsed time between target's indication in green and hitting this target. The stroke rate was calculated by the mean number of correct targets hits of the four targets pools and the mean completion time of the target pools. For analyzing the performance we evaluated a total of 646 correct target hits with a mean of 12.92 (SD = 2.51) as the average number of hits over the target pools that were collected under the gravity levels 1*g*, 1.5*g*, 1.8*g* and 2.5*g*. Entering the targets resulted in a mean stroke rate of 0.675 s^{-1} (SD = 0.085) and one target was hit with an overall mean response time of 1309.00 ms (SD = 204.07). For false target hits we evaluated a total of 43 (M = 0.86, SD = 1.25) with a mean percentage error rate of 6.14% (SD = 8.38).

Figure 4 mirrors the distribution of the frequencies of correct target hits of the three target sizing techniques (ST) per gravity level. It shows that pointing towards elongated targets (SE) results in average most correct target hits under the gravity levels 1.5*g* and 1.8*g*. In contrast, the compressed sizing technique (SC) led to the lowest number of correct target hits. Table 1 shows that pointing towards elongated SE targets also results in the fastest response time under the +Gz load 1.5*g,* as well as in the lowest percentage error rate and the highest stroke rate under the +Gz loads 1.5*g* and 1.8*g*. The pointing performance under 2.5*g* led to lowest error rate and the highest stroke rate with the normal sized technique (SU) and to the fastest response time with the compressed sizing technique (SC). Otherwise, the pointing performance with the SC method was most deteriorated under the +Gz loads 1.5*g* and 1.8*g*.

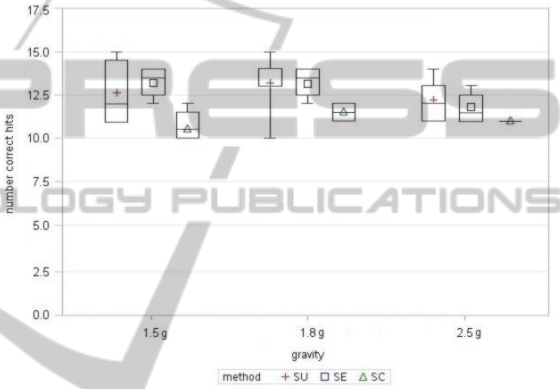

Figure 4: Distributional characteristics of frequencies of correct target hits by sizing technique per gravity load.

Table 1: Performance metrics of the LAHC case study.

ST	**Response time** (ms)	**Error rate** (%)	**Stroke rate** (s^{-1})
	mean ± SD	mean ± SD	mean ± SD
Gz = 1.5*g*			
SU	1367.25 ± 217.33	10.95 ± 5.87	0.649 ± 0.086
SC	1483.18 ± 260.69	10.21 ± 9.05	0.601 ± 0.043
SE	**1341.46** ± 81.74	**0.00** ± 0.00	**0.714** ± 0.048
Gz = 1.8*g*			
SU	**1300.01** ± 166.84	2.03 ± 3.79	0.702 ± 0.079
SC	1338.24 ± 181.74	7.28 ± 10.11	0.622 ± 0.027
SE	1312.80 ± 133.50	**1.67** ± 3.33	**0.710** ± 0.049
Gz = 2.5*g*			
SU	1322.43 ± 256.35	**4.49** ± 6.11	**0.659** ± 0.053
SC	**1239.52** ± 168.98	19.41 ± 3.49	0.585 ± 0.009
SE	1389.13 ± 166.74	14.02 ± 16.23	0.627 ± 0.054

For statistical analysis of the sizing methods over all and on same Gz load we used proc mixed (SAS® 9.4) with lsmeans/adjust = simulate to keep the experiment-wise error rate $\alpha = 0.05$. The test showed significant differences for correct and false target hits between the sizing techniques. The comparison of correct target hits revealed effects on the sizing method that indicated that scores compared with the compressed method SC (M =

11.09, SD = 0.70) were significant higher for the normal sized method SU (M = 12.65, SD = 1.47, $p = 0.0048$) and the elongated method SE (M = 12.75, SD = 1.14, $p = 0.0068$). The comparison of false target hits also revealed an effect on the sizing method that shows that the performance with the compressed method SC (M = 1.73, SD = 1.35) were significant decreased ($p = 0.0119$) compared with the normal sized method SU (M = 0.57, SD = 0.73). Overall, the case study showed that gravity-adapted target resizing and positioning significantly impacts aimed pointing performance under increased Gz loads and shows an up-coming trend for the elongated method SE.

4 USER STUDY BY ARM WEIGHTINGS

To verify the observed effect of the case study using the LAHC we performed a subsequent experiment under normogravity condition. For simulation the +Gz loads we used corresponding weightings (Guardiera et al., 2008) that were balanced attached to the participant's dominant forearm (see Fig. 5). The extended arm weights (see Table 2) were calculated (Eq. 6) for each participant as follows:

$$\boldsymbol{m_{add} = (G_{sim} - G) * \frac{m_{body}}{100} * 5.38\,\%} \qquad (6)$$

with G_{sim} for the simulated gravity force, m_{body} for the body weight of the participant and 5.38% as averaged percentage arm weights introduced by Clauser et al. (1969).

Table 2: Weights of body, arm and the added weight.

Participant	m_{body} (kg)	m_{arm} (kg)	m_{add} (kg)		
			1.5*g*	**2*g***	**2.3*g***
S1	80.0	4.3	2.2	4.3	5.6
S2	78.0	4.2	2.1	4.2	5.5
S3	75.0	4.0	2.0	4.0	5.3
S4	80.0	4.3	2.2	4.3	5.6
S5	65.0	3.5	1.8	3.5	4.6
S6	69.0	3.7	1.9	3.7	4.8
S7	60.0	3.3	1.7	3.3	4.3
S8	78.0	4.2	2.1	4.2	5.5

4.1 Apparatus

We used the same HMD setup as for the LAHC study (see section 3.1). Also all participants performed an eye-sensor calibration (Kato et al., 1999) immediately before the experiment. To perform the task of pointing towards outside coded targets, the participant stood in front of a wall with

Figure 5: Participant sitting in the LAHC cabin, wearing the OST-HMD and pointing toward the panel *(left)*. The soft-AR keyboard (*right*).

50 cm distance. We horizontal aligned the multi-pattern depending on participant's body height. The optical sensor captured the pose data with a mean frame rate of 38.52 fps (SD = 12.54). In order to assess the physiological and cognitive workload by the HRV, the participant was wearing a wireless eMotion HRV sensor from Mega Electronic (see Fig. 5, right). The HRV sensor recorded the HRV and 3-axis acceleration at a sampling frequency of 1000 Hz and an accuracy of 1 ms.

4.2 Experiment Task

To evaluate the speed-accuracy tradeoff related to Fitts' law we decided to use an appropriate task and designed a multi-directional pointing task as proposed by the ISO/DIS 9241-9 standard (2000). Therefore eight squared targets with a default size of $a = 15.0\,mm$ have been used (see Fig. 6). The targets were arranged in a circle with a default diameter of $d = 82.5\,mm$. Like the LAHC task, the participant should point towards the targets in response to visual stimuli. For evaluation purposes by Fitts' law we defined "true" target connections of 0°, 45°, 90° that implied same target distance and involves horizontal and vertical arm movements. The remaining target connections were used for pointing transition only.

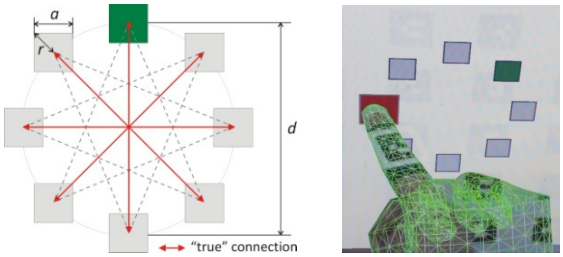

Figure 6: Multi-directional task of the weight study.

4.3 Participants

Participants were 6 male and 2 women aged 24 to 51

years (20-31 years: 4 participants, 40-51 years: 4 participants, M = 37.25, SD = 10.55). Seven participants had experiences with AR interfaces in terms of participation in previous studies and one participant was novice. They came from backgrounds in biology, physiology, aerospace and medicine. All participants had a right-dominant arm that was used for the pointing task.

4.4 Procedure and Study Design

The study consists of three independent variables (SU, SC, SE) on three +Gz loads (1.5*g*, 2*g*, 2.3*g*), with SU used as baseline condition. In a within-subject design, each participant performed the test series for all independent variables under all loads, resulting in a factorial design of 3 x 3. The repetition rate for each method amounted to five target pools per Gz load. Thereby a target pool was specified as predefined series of randomized target connection of the multi-directional pointing tasks. Pointing towards the targets of one target pool should be completed by the participants in 25 seconds. Overall each participant performed 50 test series. The multi-directional task was performed under the following order of Gz loads: 2.3*g*, 1.5*g* and 2*g*. We used systematic variations of the presentation order of the sizing methods per Gz load. Corresponding to the LAHC study we applied a fixed operation timer with 25 seconds running time and a variable participant timer that was automatically started after hitting the first target. To avoid transition effects between pool changes the first and the last signaled targets performance were not recorded. Between changes of the Gz load, the participant had a five minute break for physiological regeneration and to avoid learning effects. To be familiar with the pointing task and to check the integrity of the tracking operation, the participant undertook a short training session before starting the first condition.

4.5 Results

The participants performed the pointing task under all gravity levels using all sizing techniques. Each participant performed the eye-sensor calibration directly before starting the experiment. Table 3 presents the resulted target sizes a with its surrounding radius $r_s = \frac{a\sqrt{2}}{2}$ and targets' distance d to each other calculated by our force-based resizing approach using the active Gz load. The distance reflects the pointing range between two "true" target connections. While pointing towards normal sized target (SE) always results in same target sizes and distances at all Gz loads, the elongated sizing technique (SE) results in increased sizes and distances on increased Gz loads and contrary for the compressed technique (SC). The pointing performance was measured by the number of correct and incorrect pointing, the Euclidean distance between the target's center and the final intersection point, as well as the response time and speed of hitting a target. We also present the resulted percentage pointing error rate, the stroke rate per second and the percentage pointing accuracy. For statistical analysis the performance of the sizing techniques over all and on same Gz load, we used proc mixed (SAS® 9.4) with lsmeans/adjust = simulate to keep the experiment-wise error rate $\alpha = 0.05$. For analyzing the pointing response time and speed we only considered target hits with "true" target connections that implicated the same pointing distance per Gz load and sizing technique. Additionally we evaluated the speed-accuracy tradeoff of the sizing methods according to Fitts' law and present the movement time (MT) and throughput (TP). To evaluate the physiological strain by HRV, we assessed the R-R distance, which is the time interval in milliseconds between two heartbeats. Therefore, the R-R interval shows the impact to the cardiovascular system on a certain workload. Larger workload caused a larger impact in the cardiovascular system and causes therefore a higher heart frequency and thus a shorter R-R interval between the heartbeats.

Table 3: Resulted target size a, radius r_s and distance d.

	Gz	a (mm)	r_S (mm)	d (mm)
SU	-	15.00	10.61	82.50
SC	1.5	11.67	8.25	64.17
	2.0	10.56	7.45	58.06
	2.3	9.89	6.99	54.39
SE	1.5	18.33	12.96	100.83
	2.0	19.44	13.75	106.94
	2.3	20.11	14.22	110.61

4.5.1 Performance

Pointing Frequencies: The participants performed the task with 5 repetitions under 10 paired conditions with a total of 50 trials per participant. A single task was timed to 25 seconds where the participant tried to hit signalled targets. Overall, the participants pointed towards 6708 targets (SU = 30.7 % , SC = 32.3 %, SE = 37.0 %) in a correct way and towards 102 targets (SU = 33.7 %, SC = 34.7 %, SE = 31.6 %) in a wrong way. Within 25 seconds (i.e. one target pool) the average frequency of correct target hits was 19.39 (SD = 3.37) and of false hits

0.27 (SD = 0.66). Table 4 splits this into the interaction effect of the Gz loads on the studied sizing techniques (SU, SC, SC) and additionally shows the corresponding average frequency of incorrect target hits, percentage error rate and hit rate per second. Examining the three sizing techniques per increased Gz load (1.5*g*, 2*g*, 2.3*g*) data reveals that all means of the elongated sizing technique (SE) are higher (correct hits, stroke rate) or lower (incorrect hits, error rate) under 2*g* and 2.3*g* than the SU and SC technique. Under 1.5*g* the compressed method (SC) resulted in higher mean values for correct hits and the stroke rate, and the unchanged technique (SU) in lower means for incorrect pointing. The distributional characteristics for correct target hits are featured in Figure 7.

Table 4: Performance metrics of the arm weightings study: number correct and false hits, error and stroke rate.

ST	Correct hits	False hits	Error (%)	Stroke (s^{-1})
	mean ± SD	mean ± SD	mean ± SD	mean ± SD
Gz = 1.5*g*				
SU	20.70 ± 2.63	**0.09** ± 0.43	**0.53** ± 2.44	0.88 ± 0.11
SC	**21.20** ± 2.76	0.13 ± 0.34	0.70 ± 1.92	**0.91** ± 0.08
SE	21.07 ± 2.30	0.13 ± 0.34	0.66 ± 1.71	0.89 ± 0.09
Gz = 2.0*g*				
SU	17.56 ± 4.22	0.40 ± 0.82	2.69 ± 5.51	0.75 ± 0.16
SC	18.31 ± 4.37	0.26 ± 0.66	1.85 ± 5.41	0.78 ± 0.18
SE	**19.85** ± 2.48	**0.18** ± 0.45	**1.04** ± 2.58	**0.85** ± 0.09
Gz = 2.3*g*				
SU	18.45 ± 3.57	0.46 ± 0.88	2.40 ± 4.67	0.79 ± 0.10
SC	16.88 ± 3.84	0.48 ± 0.85	2.89 ± 5.16	0.73 ± 0.16
SE	**18.95** ± 2.36	**0.43** ± 0.87	**2.23** ± 4.69	**0.80** ± 0.10

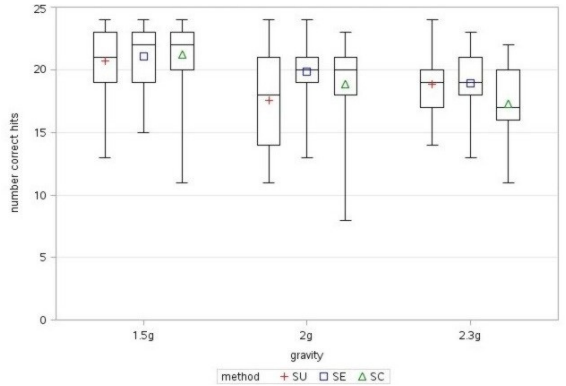

Figure 7: Distributional characteristics of correct target hits by sizing technique per gravity load.

In terms of differences between the correct hits of the sizing techniques over all Gz loads showed an significant improvement (see Table 5) of the performance using the elongated sizing technique SE (M = 20.00, SD = 2.53) compared to the normal sizing technique SU (M = 19.05, SD = 3.52, p = *0.0373*) and to the compressed sizing technique SC (M = 18.82, SD = 4.09, p = *0.0141*).

Table 5: Significant differences of correct pointing using SAS proc mixed with lsmeans/adjust=simulate.

Effect	ST	Gz	ST	Gz	Estima.	StdErr	DF	Adj P
ST	SE	-	SU	-	1.052	0.426	338	0.0373
ST	SE	-	SC	-	-1.158	0.413	338	0.0141

Accuracy: The pointing accuracy reflects the precision of target pointing and was measured by the Euclidean distance d_{ED} and the surrounding radius r_s of the targets (see Table 3). The distance d_{ED} is the distance between the centre of the target and the intersection point within the target. Table 6 presents amongst others the means and standard deviations (SD) of the distance d_{ED} and the percentage accuracy of the sizing techniques per Gz load.

Table 6: Euclidean distance, accuracy, response time and speed of the sizing techniques (ST) per Gz load.

ST	d_{ED} (mm)	Accuracy (%)	Response time (ms)	Speed (mm/ms)
	mean ± SD	mean ± SD	mean ± SD	mean ± SD
Gz = 1.5*g*				
SU	4.23 ± 2.49	**60.10** ± 23.46	**1007.35** ± 173.11	0.085 ± 0.017
SC	**3.58** ± 1.96	56.59 ± 23.71	1016.00 ± 173.11	0.065 ± 0.012
SE	5.38 ± 2.99	58.51 ± 23.13	1029.43 ± 164.93	**0.101** ± 0.018
Gz = 2.0*g*				
SU	4.78 ± 2.74	54.93 ± 25.79	**1012.15** ± 195.92	0.085 ± 0.019
SC	**3.80** ± 1.87	49.13 ± 24.99	1039.77 ± 202.71	0.058 ± 0.012
SE	5.85 ± 3.34	**57.47** ± 24.30	1031.43 ± 152.39	**0.106** ± 0.017
Gz = 2.3*g*				
SU	5.02 ± 2.50	52.72 ± 23.58	1073.56 ± 184.71	0.079 ± 0.015
SC	**3.36** ± 1.71	51.94 ± 24.45	**1068.76** ± 210.42	0.053 ± 0.012
SE	5.65 ± 3.14	**60.24** ± 22.09	1078.08 ± 159.12	**0.105** ± 0.016

The graphical distribution of the Euclidean distances are presented in Figure 8 and shows a proportional ratio between the distance and target's size, i.e. the pointing distance is greater with the increment of target's size and vice versa. The statistical analyzing of the Euclidean distance confirmed this observation by significant differences between the sizing techniques. The test revealed that pointing towards SC targets (M = 3.56 mm, SD = 1.96) resulted in significant shorter distances analyzed over all Gz loads (p < *.0001*) compared to SU (M = 4.56 mm, SD = 2.56) and SE (M = 5.61 mm, SD = 3.15). But it also showed differences (p < *.0001*) for grouped effects (ST*Gz) by comparing the sizing techniques on same Gz stage.

In contrast, the accuracy (see Fig. 9) mirrors the percentage ratio of the distance d_{ED} to the target size expressed by the radius r_s. The participants pointed with an overall mean percentage accuracy of 56.39 %. Per sizing technique over all Gz loads data

revealed that relative to target's size, participants more precise pointed using the elongated method (SE) with 58.72 % accuracy (SU: 56.77 %, SC: 53.19 %). Statistical analyzing (see Table 7) revealed that pointing towards elongated targets (SE) enabled a significant improvement ($p < .0001$) compared to pointing towards compressed targets (SC) over all Gz loads and separated by comparison on same Gz stage, revealed in significant differences under 2*g* ($p < 0.0178$) and 2.3*g* ($p < 0.0072$). The comparison between pointing towards elongated (SE) and normal sized targets (SU) resulted in significant improvement under 2.3*g* ($p < 0.0436$) using the SE sizing technique.

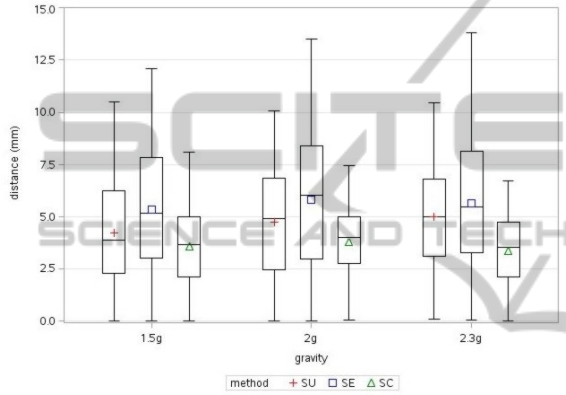

Figure 8: Distributional characteristics of Euclidean distance by sizing technique per gravity load.

Table 7: Significant differences of accuracy using SAS proc mixed with lsmeans/adjust=simulate.

Effect	ST	Gz	ST	Gz	Estima.	StdErr	DF	Adj P
ST	SE	-	SC	-	-6.185	1.292	1951	< .0001
ST*Gz	SE	2.0	SC	2.0	-8.341	2.434	1951	0.0178
ST*Gz	SE	2.3	SC	2.3	-8.303	2.255	1951	0.0072
ST*Gz	SE	2.3	SU	2.3	7.518	2.392	1951	0.0436

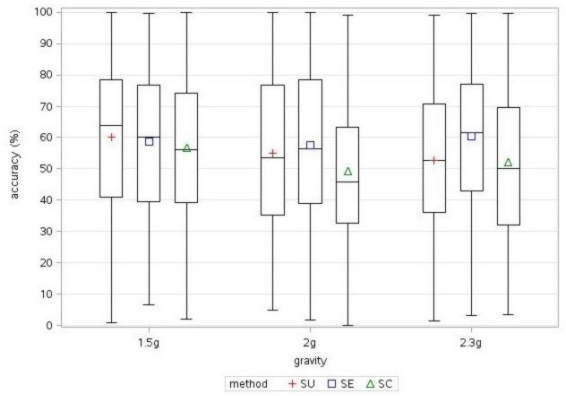

Figure 9: Distributional characteristics of accuracy by sizing technique per gravity load.

Response Time: The response time (in millisecond) is the time between highlighting a target and selecting this target by the index finger. The means and standard deviations (SD) are showed in Table 6. Overall the participants pointed with a mean response time of 1038.60 ms (SD = 179.26). Only considering the sizing techniques at summarized Gz loads data revealed shorter response times for pointing towards normal sized target (SU) with a mean of 1028.62 ms (SD = 183.49) compared to compressed targets using the SC method (M = 1039.99 ms, SD = 195.32) and elongated targets using the SE method (M = 1044.75 ms, SD = 160.75). The distribution of the response time for the sizing techniques per Gz load is presented in Figure 10. Longest response times, but not significant, were achieved using the elongated method (SE) under 1.5*g* and 2.3*g*. This is contrary to our expectation of significant longer response times at larger target distances (SE) under all Gz loads

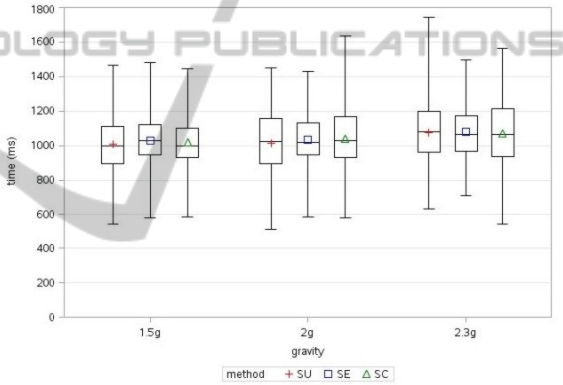

Figure 10: Distributional characteristics of response time by sizing method per gravity load.

Pointing Speed: The speed (in mm/ms) was calculated by the distance between the targets (see Table 3) divided by the response time. The means and standard deviations (SD) are also presented in Table 6. Because targets' size and distance varies with the used sizing technique and the Gz load, analyzing the speed is more meaningful than the response time. Overall the participants pointed with a mean speed of 0.083 mm/ms (SD = 0.024). The distribution of pointing speed by the sizing technique per gravity load is presented in Figure 11.
In contrast to the resulted response times, with significant higher speed was pointed towards elongated targets (SE) that were placed with greater distances to each other. In Table 8 we are presenting significant differences that shows a significant improvement with $p < .0001$ for the SE method (M = 0.104, SD = 0.017) analyzed over all Gz loads at

comparing with the other two sizing methods (**SU:** M = 0.083, SD = 0.017, **SC:** M = 0.059, SD = 0.013), and shows significant faster pointing using the SE methods ($p < .0001$) for grouped effects (ST*Gz) by comparing the sizing techniques on same stage of the Gz load.

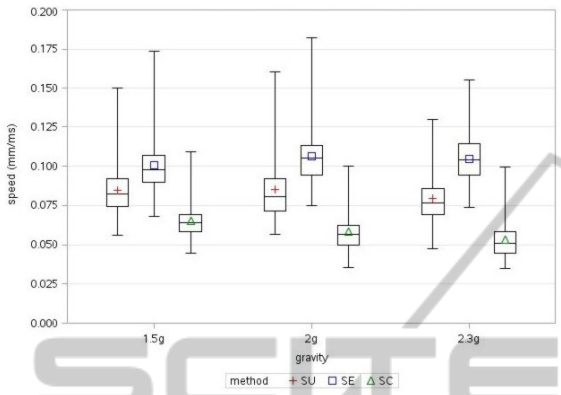

Figure 11: Distributional characteristics of pointing speed by sizing technique per gravity load. (*$p < .05$).

Table 8: Significant differences of pointing speed using SAS proc mixed with lsmeans/adjust=simulate.

Effect	ST	Gz	ST	Gz	Estima.	StdErr	DF	Adj P
ST	SE	-	SC	-	-0.0451	0.00081	2046	< .0001
ST	SE	-	SU	-	0.0209	0.00088	2046	< .0001
ST	SC	-	SU	-	-0.0242	0.00091	2046	< .0001
ST*Gz	SE	1.5	SC	1.5	-0.0355	0.00128	2046	< .0001
ST*Gz	SE	2.0	SC	2.0	-0.0480	0.00150	2046	< .0001
ST*Gz	SE	2.3	SC	2.3	-0.0518	0.00143	2046	< .0001
ST*Gz	SE	1.5	SU	1.5	0.0161	0.00126	2046	< .0001
ST*Gz	SE	2.0	SU	2.0	0.0211	0.00175	2046	< .0001
ST*Gz	SE	2.3	SU	2.3	0.0256	0.00152	2046	< .0001
ST*Gz	SC	1.5	SU	1.5	-0.0195	0.00131	2046	< .0001
ST*Gz	SC	2.0	SU	2.0	-0.0269	0.00183	2046	< .0001
ST*Gz	SC	2.3	SU	2.3	-0.0262	0.00155	2046	< .0001

4.5.2 Fitts' Law

In designing Human-Computer-Interfaces the assessment of ergonomics is mainly determined by Fitts' model of movement time (Eq. 7) (Fitts, 1954) that a human needs to point at a target of a given size and distance. Fitts' law predicts longer movement times at larger distances, as well as at smaller targets. Our sizing approach interrelates this characteristics to each other, whereby the elongated method (SE) provides larger targets at larger distances, while the compressed method (SC) results in smaller targets at smaller distances. We used Fitts' law to evaluate the speed-accuracy trade-off of the studied sizing techniques related to direct pointing affected by added arm weightings. The metric for comparing the performance is the Throughput *TP* (Eq. 8), in bits per second (bps) calculated by the Index of Difficulty *ID* and mean movement time *MT* (Eq. 8) as time to hit a target in millisecond with a for the intercept and b for the slope of measured mean response time by the target width *W*. The *ID* measures the tasks difficulty in bits using target size and distance. Because we used squared targets, we calculated the *ID* only by the targets' width. For computing the *ID* (Eq. 9) we used the Welford formulation (Welford, 1960). To reflect the observed pointing performance of the participants, we used the effective target width W_e (Eq. 10) (MacKenzie, 1992; Welford, 1960) as the central 96 % of the spatial distribution with SD_x as standard deviation of the mean pointing accuracy.

$$MT = a + b\,ID_e \tag{7}$$

$$TP = \frac{ID_e}{MT} \tag{8}$$

$$ID_e = \log_2\left(\frac{A}{W_e} + 0.5\right) \tag{9}$$

$$W_e = 4.133 * SD_x \tag{10}$$

Table 9 shows the resulting Fitts' parameter for the three sizing methods per +Gz load. The SE method resulted overall in the highest ID_e and therefore in most difficult targets, but also in the highest throughput (*TP*). The compressed sizing method (SC) yielded the highest index of difficulty under 1.5*g*, but under 2*g* and 2.3*g* yielded most simple targets. Pointing towards normal sized targets (SU) yielded increased ID_e, as well as a growing throughput with the increment of gravity. Two-Way analysis of variance did not show significant effects between the methods' throughputs ($F_{2,4} = 1.52$, $p > .05$).

Table 9: Fitts' resulted parameters: targets' distance (A), target width (W), effective target width (W_e), mean measured movement time (MT), effective Index of Difficulty (ID_e), and Throughput (TP).

	+Gz	A (mm)	W (mm)	W_e (mm)	MT (ms)	ID_e (bits)	TP (bps)
SU	1.5	82.50	15.00	14.47	1010.61	**2.63**	**2.61**
	2.0	82.50	15.00	11.04	1052.83	**2.99**	**2.85**
	2.3	82.50	15.00	11.78	1071.96	**2.91**	**2.71**
SC	1.5	64.17	11.67	8.47	1021.53	**3.02**	**2.96**
	2.0	58.06	10.56	11.12	1032.42	**2.52**	**2.44**
	2.3	54.39	9.89	9.09	1085.23	**2.69**	**2.49**
SE	1.5	100.83	18.33	13.68	1029.36	**2.98**	**2.89**
	2.0	106.94	19.44	13.39	1035.30	**3.09**	**2.98**
	2.3	110.61	20.11	13.18	1089.69	**3.15**	**2.89**

The resulting Pearson's correlation coefficient *r* and the regression equations of Fitts' movements model for the sizing conditions are presented in Table 10. While the movement time and the index of difficulty

highly linear correlate ($r > 8.0$) for the SU and SE conditions, a low correlation was yielded from the SC condition. The Fitts' model of movement time of the SU (Eq. 11) and SE (Eq. 13) sizing conditions provides good descriptions of the observed pointing behaviour. Contrary to this, the model of the compressed sizing technique SC (Eq. 12) resulted in a model with a high intercept at a negative slope, i.e. that the Movement Time is decreased for an increased Index of Difficulty and vice versa. The high intercept implies a movement time of 1.163 s at $ID = 0$ bits that is about twice the *MT* of the SU condition and about 14-fold of SE's *MT*.

Table 10: Pearson's correlation coefficient *r* between *MT* and ID_e, and linear regression equation of Fitts' model of *MT* per sizing technique over increased Gz loads.

	r	**Fitts' model of movement time** (ms)	
SU	0.856	$MT = 638 + 142\ ID_e$	(11)
SC	-0.321	$MT = 1163 - 43\ ID_e$	(12)
SE	0.842	$MT = 81 + 315\ ID_e$	(13)

4.5.3 Physiological Workload

The cardiovascular parameters were assessed during all phases of the experiment. The 1*g* SU output was used as reference measurement and showed the lowest impact on the cardiovascular system. Since the physiological workload grows with the increment of gravity respectively the weight and R-R distance (see Table 11) decreases during the experiment under 2*g* and even more under 2.3*g*. The R-R distances are showing the lowest values for the SU, SC and SE conditions under high Gz load since the weight attached to the participants' arm constituted the major part of the workload. While pointing towards elongated SE targets (largest target distances) yielded the lowest values for the R-R distances under all Gz loads, pointing towards compressed SC targets (smallest target distances) resulted in the highest values for the R-R distance and therefore in the lowest workload. Two-Way analysis of variance showed a significant effect between the R-R distance produced by increased Gz loads ($F_{2,4} = 27.69$, $p < .05$), but did not show effects by the sizing methods ($F_{2,4} = 4.21$, $p > .05$).

Table 11: Assessed HRV parameters: R-R distance in [ms] median and SD across all participants.

Gz	SU	SC	SE
1.0	723,86 ± 156.88	-	-
1.5	674,24 ± 114.76	680,45 ±120.29	665,09 ± 102.56
2.0	**642,11 ± 119.43**	**649,57 ±117.03**	**625,28 ± 88.07**
2.3	**641,97 ± 105.77**	**648,31 ±119.25**	**645,24 ± 126.40**

5 DISCUSSION

While the LAHC study has already shown a small effect of gravity-based sizing, the weight study has confirmed that the performance and workload during AR selection is influenced by the online adaptation of changed gravity load to the size and position of the virtual information. The weight study also confirmed and verified the observed trend of an improved performance of pointing towards targets influenced by the present gravity load in an elongated fashion (greater size, larger distance). The results showed an overall significant increment of the pointing frequencies towards elongated targets, accompanied by a likewise non-significant decrement of the error rate under 2*g* and 2.3*g*. In contrast to elongated targets, the compressed sizing technique yields the smallest targets at short distances. This enables significant closer hits to the targets' centre. Conversely, pointing towards elongated targets ensures significant most precise pointing relative to targets sizes. The most important finding revealed that larger targets at greater distances between the targets calculated by the active Gz load significantly accelerates the pointing performance. Conversely, the results showed that pointing towards compressed targets (smaller size, shorter distance) generates the opposite effect resulting in decreased performance. Also the analysis of the speed-accuracy tradeoff related to Fitts' law yielded in a higher, but not significantly, throughput by larger target size and distance. The HRV based parameters showed an effect caused by changed gravity respectively for attached arm weights and the alternation of the workload. Therefore, the assessment of workload during the application of AR, by measuring cardiovascular parameters such as the HRV, is a promising method to improve the user performance in normogravity and altered gravity.

6 CONCLUSION AND FUTURE WORK

We conducted a proof-of-concept study to investigate the influence of the online adaption of the present gravity load to target size and distance on direct AR pointing. Two experimentations were performed by simulated hypergravity induced by long-arm human centrifugation and by added arm weightings under normogravity. In conclusion, our results are showing that direct AR pointing under changed gravity conditions is impacted by adapted target size, as well as the distance between the targets. Under increased Gz loads the pointing performance benefits from increased sizes and distances depending on the Gz load. This is a promising direction for further HCI research. Our next step will be the adaptation of the experiment to

the corresponding investigation under microgravity conditions. In further research we will replace direct fingertip pointing by gaze-based selection for more adequate fitting the AR view management of our future AR supported assistant system for space operation procedures. Related to the HRV, for the next step we will consider separating physical and cognitive workload by assessing the muscular activity and applying electromyogram (EMG) to the participant's weighted arm. By doing that we could even more precisely assess the workload during pointing and targeting.

REFERENCES

Agan, M., Voisinet, L. A., Devereaux, A.. 1998. NASA's Wireless Augmented Reality Prototype (WARP). In *Proc. of AIP'98*, pp. 236-242, 1998.

Azuma, R.T. 1997. A survey of augmented reality. In *Presence, Teleopera-tors and Virtual Environments*, vol. 6, no. 4, pp. 355–385.

Bock, O., Howard, I. P., Money, K. E., Arnold, K. E. 1992. Accuracy of aimed arm movements in changed gravity. In *Aviation, Space, and Environmental Medicine*, vol. 63, pp. 994-998.

Bock, O. 1998. Problems of sensorimotor coordination in weightlessness. In *Brain Research Reviews*, vol. 28, pp. 155-160.

Clauser, C. E., McConville, J. T., Young, J. W. 1969. Weight, volume, and center of mass of segments of the human body. AMRL Technical Report 69-70. Wright-Patterson Air Force Base.

Department of Defense. 1999. Design criteria standard, human engineering. Technical Report MIL-STD-1472F.

Fisk, J., Lackne, J. R., DiZio, P. 1993. Gravitoinertial force level influences arm movement control. In *Journal of Neurophysiology*, vol. 69, pp. 504-511.

Fitts, P.M. 1954. The Information Capacity of the Human Motor System in Controlling the Amplitude of Movement. In *Journal of Experimental Psychology*, 47 pp. 381-391.

Guardiera, S., Schneider, S., Noppe, A., Strüder, H. K. 2008. Motor performance and motor learning in sustained +3Gz acceleration. In *Aviation Space and Environmental Medicine*, vol. 79(9), pp. 852-9.

Hartmann, K., Ali, K., Strothotte, T. 2004. Floating Labels. Applying Dynamic Potential Fields for Label Layout. In *Smart Graphics*, vol. 3031, Springer, pp. 101–113.

ISO/DIS 9241-9. 2000. Ergonomic requirements for office work with visual display terminals (VDTs) - Part 9: Requirements for non-keyboard input devices. International Standard, International Organization for Standardization.

Kato, H., Billinghurst, M. 1999. Marker Tracking and HMD calibration for a video-based augmented reality conferencing system. In *Proc. IWAR'99*, vol. 0, pp. 85-94.

Kohli, L., Whitton, M. C., Brooks, F. P. 2012. Redirected touching: The effect of warping space on task performance. In *Proc of 3DUI'12*, pp. 105-112.

Looser, J., Billinghurst, M., Grasset, R., Cockburn, A. 2007. An evaluation of virtual lenses for object selection in augmented reality. In *Proc of. GRAPHITE'07*, pp. 203-210.

MacKenzie, I. S. 1992. Fitts' law as a research and design tool in human-computer interaction. In *Journal of Human-Computer Interaction*, vol. 7, pp. 91–139.

Markov-Vetter, D., Moll, E., Staadt O. 2012. Evaluation of 3D Selection Tasks in Parabolic Flight Conditions: Pointing Task in Augmented Reality User Interfaces. In *Proc. of VRCAI'12*, pp.287-293.

Markov-Vetter, D., Zander, V., Latsch, J. Staadt, O. 2013. The Impact of Altered Gravitation on Performance and Workload of Augmented Reality Hand-Eye-Coordination: Inside vs. Outside of Human Body Frame of Reference. In *Proc. of JVRC'13*, pp. 65-72.

Oehme, O., Schmidt, L., Luczak, H. 2002. Comparison between the strain indicator hrv of a head based virtual retinal display and lc-mounted displays for augmented reality. In *Proc. of WWDU '02*, pp. 387-389.

Pick, S., Hentschel, B., Tedjo-Palczynski, I., Wolter, M., Kuhlen, T. 2010. Automated positioning of annotations in immersive virtual environments. In *Proc. of JVRC'10*, pp. 1-8.

Rohs, M., Oulasvirta, A., Suomalainen, T. 2011. Interaction with magic lenses: real-world validation of a Fitts' Law model. In *Proc. of CHI'11*, pp. 2725-2728.

Scheid, F., Nitsch, A., König, H., Arguello, L., De Weerdt, D., Arndt, D., Rakers, S. 2010. Operation of European SDTO at Col-CC. *SpaceOps 2010 Conference*.

Task Force of the European Society of Cardiology and the North American Society of Pacing and Electrophysiology. Heart Rate Variability: standards of measurement, physiological interpretation and clinical use. 1996. Circulation 1996 (93) 1043-1065 / Eur Heart J, 17(3):354-81.

Tümler, J., Mecke, R., Schenk, M., Huckauf, A., Doil, F., Paul, G., Pfister, E., Böckelmann, I., Roggentin, A. 2008. Mobile Augmented Reality in Industrial Applications: Approaches for Solution of User-Related Issues. In *Proc. of ISMAR'08*, pp. 87-90.

Welford, A. T. 1960. The measurement of sensory-motor performance: Survey and reappraisal of twelve years' progress. In *Ergonomics*, 3, 189-230.